Mitochondrial ''swirls'' induced by oxygen stress and in the *Drosophila* mutant *hyperswirl*

David W. Walker and Seymour Benzer*

Division of Biology, California Institute of Technology, Pasadena, CA 91125

Mitochondrial dysfunction and reactive oxygen species have been implicated in the aging process as well as a wide range of hereditary and age-related diseases. Identifying primary events that result from acute oxidative stress may provide targets for therapeutic interventions that preclude aging. By using electron microscopy, we have discovered a striking initial pattern of degeneration of the mitochondria in *Drosophila* flight muscle under hyperoxia (100% O$_2$). Within individual mitochondria, the cristae become locally rearranged in a pattern that we have termed a ''swirl.'' Serial sections through individual mitochondria reveal the reorganization of the cristae in three dimensions. The cristae involved in a swirl are deficient in respiratory enzyme cytochrome *c* oxidase activity, within an otherwise cytochrome *c* oxidase-positive mitochondrion. In addition, under hyperoxia cytochrome *c* undergoes a conformational change, manifested by display of an otherwise hidden epitope. The conformational change is correlated with widespread apoptotic cell death in the flight muscle, as revealed by *in situ* terminal deoxynucleotidyltransferase-mediated dUTP nick end labeling. In normal flies, mitochondrial swirls accumulate slowly with age. To investigate the molecular mechanisms involved in oxygen toxicity, we conducted a genetic screen for mutants that display altered survival under hyperoxia, and we identified both sensitive and resistant mutants. We describe a mutant, *hyperswirl*, which displays an overabundance of swirls with associated respiratory and flight defects and a greatly reduced lifespan. Such mutants can identify genes that are needed to maintain mitochondrial homeostasis throughout the lifespan.

hyperoxia | aging | cytochrome *c* | apoptosis | muscle

Molecular oxygen is a biradical that, upon single electron addition, sequentially generates O$_2^-$, H$_2$O$_2$, and ·OH, which, by means of further reactions, can generate an array of additional reactive oxygen species (ROS). D. Harman (1) proposed that free radicals produced during aerobic respiration cause cumulative oxidative damage, resulting in aging and death. Several lines of evidence that support this hypothesis have been established (2–4). It has been shown that ROS can damage cellular macromolecules, including DNA, lipids, and proteins (5–8). Mutations that lead to extended lifespan have been identified in yeast, worm, fly, and mouse, and there is a correlation between increased longevity and enhanced resistance to oxidative stress in these mutants (9, 10). Treatment of WT *Caenorhabditis elegans* with synthetic superoxide dismutase/catalase mimetics increases the mean lifespan by 44% (11), providing direct evidence for the role of oxygen radicals in determining the aging rate in the nematode. In *Drosophila*, transgenic technology has been used to directly test the free-radical theory of aging. Overexpression of the mitochondrial manganese superoxide dismutase significantly extends adult lifespan (12), the degree of extension in different transgenic lines being correlated with the level of manganese superoxide dismutase activity. Overexpression of copper–zinc superoxide dismutase alone, or in combination with catalase, has also been reported to increase lifespan (13–15). However, other studies (16) have reported no extension, and the reasons for the inconsistency are unclear.

The mitochondrial electron transport chain consumes 85% of the oxygen used by the cell. Therefore, a logical extension of the free-radical theory of aging focuses attention on the mitochondria. Considerable evidence supports the idea that mitochondria are a major target of the aging process (17, 18). Progressive loss of mitochondrial function is a common feature of aging in several tissues and organisms (19–21), and accumulation of deletions and point mutations in mitochondrial DNA has been described in aged individuals (22, 23). Mitochondrial dysfunction and ROS have been implicated in a wide range of age-related neurodegenerative disorders, including Alzheimer's disease and Parkinson's disease (24, 25). Also, hereditary defects in genes encoding mitochondrial components can result in chronic diseases, such as Leigh syndrome, which is characterized by spongy degeneration and capillary proliferation within the basal ganglia and presents with developmental regression, brainstem dysfunction, generalized muscle weakness, respiratory problems, poor motor function, loss of vision, and seizures (26). It has been proposed that the symptoms of mitochondrial diseases, such as Leigh syndrome, are the result of two pathophysiological effects of oxidative-phosphorylation deficiency: reduced ATP production and increased toxicity of ROS (18).

Exposure to hyperoxia (100% O$_2$) offers an attractive model for physiological studies of oxidative stress because the adverse effects are due to increased intracellular flux of ROS generated by normal metabolic pathways (27, 28). Exposure to hyperoxia has been reported to lead to degenerative changes in rodents, including cognitive impairment (29). In *C. elegans*, exposure to hyperoxia reduces lifespan significantly (30). This effect is more pronounced in the mutant *mev-1*, a gene that encodes succinate dehydrogenase cytochrome *b* (31). In the house fly, mitochondrial aconitase, an enzyme in the citric acid cycle, has been reported to be a target of hyperoxia-induced damage (32). Hyperoxia also greatly shortens the lifespan of *Drosophila* (33, 34) and has been reported to lead to degeneration of the CNS (35, 36).

To identify primary events in the aging process, we have examined the pathological consequences of hyperoxia in adult *Drosophila* by using electron microscopy. We have discovered a striking initial pattern of degeneration that occurs rapidly in mitochondria of the indirect flight muscle, a pathology that accumulates more slowly in flies aging under normoxia. The pathological lesion is in the form of a ''swirl'' within an otherwise normal mitochondrion. Swirls are associated with defects in components of the respiratory chain, specifically, localized loss of cytochrome *c* oxidase (COX) activity and a conformational change in cytochrome *c*, which is a harbinger of apoptotic cell death. In parallel, we have taken a genetic approach to identify mutants in which the effects of hyperoxia are enhanced or inhibited. The previously identified long-lived *methuselah* (*mth*) mutant (37) has enhanced resistance to hyperoxia. The previ-

---

ously uncharacterized, short-lived mutant *hyperswirl* (*hys*) is extremely sensitive to hyperoxia and displays an abundance of swirls, even under normoxia, as well as metabolic and flight defects. This approach provides a paradigm for identifying nuclear-encoded genes that regulate mitochondrial structure and function.

Methods

Fly Strains and Ab. The *Drosophila* strains *white^1118* and the WT *Canton-S* were used. Male flies were used throughout this study. We screened a publicly available collection of insertion lines containing enhancer promoter-transposable elements (38). mAb 2G8 was provided by R. Jemmerson (University of Minnesota, Minneapolis).

Exposure to Hyperoxia. Adult males (3–4 days old) in shell vials (20–25 flies per vial) covered with nylon mesh containing standard food (cornmeal/yeast/agar) were placed in a Plexiglas enclosure of $28 \times 28 \times 24$ inches at room temperature (22–24°C). Oxygen (100%) was passed through the box at a constant rate (300 ml/min).

Electron Microscopy. Dorsal indirect flight muscle from adult flies was fixed overnight at 4°C in 2% paraformaldehyde plus 1% glutaraldehyde, postfixed in 1% osmium tetroxide (OsO_4) at room temperature, dehydrated in an ethanol series, and embedded in Epon 812. Ultrathin sections (80 nm) were examined with a 420 electron microscope (Philips, Eindhoven, The Netherlands) at 100 kV.

Quantification of Swirl Frequency. To estimate the frequency of swirl formation after exposure to hyperoxia, sections of flight muscle, containing at least 80 mitochondria, were scored for swirl formation, from each of 10 individual flies of the w^{1118} strain.

COX Electron Micrographs. COX activity was assayed as described by Nonaka *et al.* (39). In brief, dissected flight muscle was fixed in 2% glutaraldehyde in PBS (0.15 NaCl/27 mM KCl/12 mM NaH_2PO_4, pH 7.2) for 10 min at 4°C. The tissue was incubated in a solution of 5 mg of 3,3′-diaminobenzidine tetrahydrochloride/9 ml of 0.05 M sodium phosphate buffer, pH 7.4/1 ml of catalase (20 μg/ml)/10 mg of cytochrome c/750 mg of sucrose, for 3 h at 37°C. The tissue was washed in PBS for 1 h and prepared for electron microscopy, as described above.

Ab Staining. Dorsal indirect flight muscle was dissected and fixed in 1% glutaraldehyde plus 1% paraformaldehyde in PBS, washed in PBS, and then permeabilized with PBS and 10% Tween 20. The tissue was stained with the mAb 2G8 at a 1:50 dilution overnight at 4°C. The tissue was incubated with goat anti-mouse IgG conjugated with horseradish peroxidase, and 3,3′-diaminobenzidine tetrahydrochloride was used to develop the horseradish peroxidase. Subsequently, samples were prepared for electron microscopy, as described above.

Terminal Deoxynucleotidyltransferase-Mediated dUTP Nick End Labeling (TUNEL). Male flies were cryo-sectioned and fixed in 4% methanol-free formaldehyde in PBS for 25 min. The sections were then subjected to TUNEL staining (Dead End, Promega) and viewed by fluorescence microscopy.

Lifespan Determination. Newly eclosed flies were maintained at 25°C in shell vials (20–25 flies per vial) containing standard food (cornmeal/yeast/agar), transferred to fresh vials (with cotton stoppers) every 2–3 days, and scored for survival.
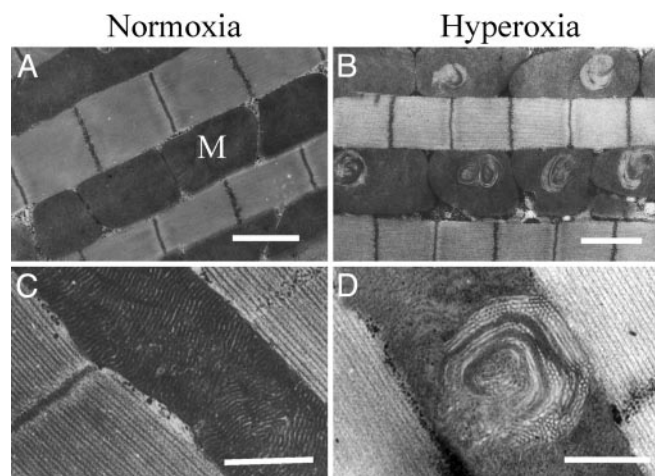

Fig. 1. Mitochondrial swirls accumulate under hyperoxia. (*A*) Electron micrograph of flight muscle of *Drosophila* (*white^1118* strain) maintained for 7 days under normoxic conditions. Mitochondria (M) are aligned between the myofibrils. (*B*) Electron micrograph of flight muscle of *Drosophila* (*white^1118* strain) after 7 days under hyperoxia (100% O_2). Mitochondrial swirls are seen in most mitochondria. (*C*) A normal mitochondrion at higher magnification. (*D*) A typical swirl at higher magnification. (Scale bars indicate 1 μm.)

Metabolic Measurements. Groups of 10 flies in 2.2-ml glass vials were assayed by using a TR-2 CO_2 gas respirometer (model LI-6251; Sable Systems International, Henderson, NV). The vial was flushed with CO_2-free air and placed in the respirometer for 5–6 h at 25°C. CO_2 production was calculated by using DATACAN software (Sable Systems International).

Flight Test. Flight capability was assayed as described in ref. 40. In brief, flies were dropped into a 500-ml graduated cylinder, in which the inside wall was coated with paraffin oil. The distribution of the levels at which the flies hit the wall and become stuck in the oil reflects their flying ability. Three independent trials, each consisting of >30 flies, were conducted on age-matched control (WT) and mutant flies.

Results

By using electron microscopy, we identified a striking degeneration of the mitochondria within the flight muscle under oxygen stress. In insect flight muscle, the mitochondria typically lie in columns, aligned longitudinally between the myofibrils (Fig. 1 *A* and *C*). The cristae within these mitochondria are packed very densely so that any changes in their configuration are easily seen. The myofibril structure in flies exposed to hyperoxia was indistinguishable from those of control flies. By contrast, mitochondria manifesting rearrangement of the cristae were a uniform feature of flies exposed to hyperoxia for ≥4 days. In the earliest event visible by electron microscopy, the cristae, in a local region within a mitochondrion, lose their tightly packed and orderly structure, generating a swirl within an otherwise normal-looking mitochondrion (Fig. 1 *B* and *D*). We examined sections, at 10-μm intervals, throughout the flight muscle, and we observed swirls distributed throughout the tissue after exposure to hyperoxia. With continued exposure to hyperoxia, there is an increase in the number of mitochondria affected. In *white^1118* flies after 4 days of exposure to hyperoxia, $35 \pm 13\%$ of the mitochondria contained swirls; after 7 days of exposure to hyperoxia, $62 \pm 8\%$ of the mitochondria contained swirls (Fig. 2). Control flies maintained under normoxia displayed a very low frequency of swirl formation (≈2% of mitochondria contained swirls).

Complex IV (COX) is the terminal enzyme in the electron transport chain. COX activity has been reported to decline with
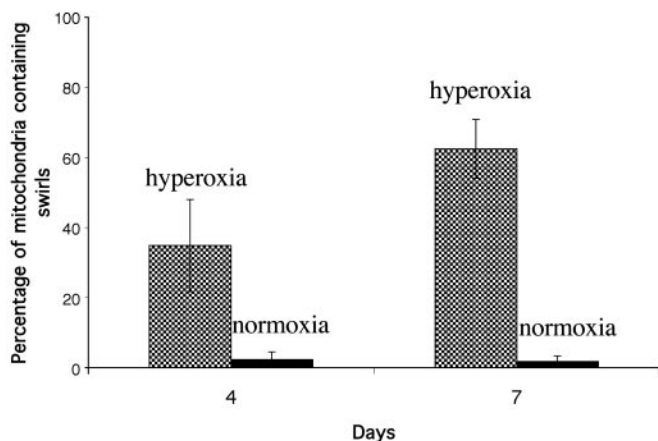
Fig. 2. Frequency of swirl formation under hyperoxia. Sections of flight muscle were examined for swirl formation after 4 and 7 days under hyperoxia. Age-matched controls were maintained under normoxia. Data are averages of 10 flies ± SD, with >80 mitochondria scored from each individual fly.

age and under oxidative stress in *Drosophila* (21). To examine the functional relevance of swirls, we used a staining technique to identify COX activity at the individual mitochondrial level. In flight muscle of control flies that had been maintained under normoxic conditions, the mitochondria displayed uniform COX activity (Fig. 3*A*). However, in flies exposed to hyperoxia, the cristae involved in a swirl were COX⁻, within an otherwise COX⁺ mitochondrion (Fig. 3*B*). The role of mitochondria and cytochrome *c*, the substrate of COX, in programmed cell death has drawn considerable attention in recent years (41). In *Drosophila*, it has been reported that an overt alteration in cytochrome *c* anticipates apoptotic cell death during development (42). The altered configuration is manifested by display of an otherwise hidden epitope, which occurs without release of the protein into the cytosol. The anti-cytochrome *c* mAb 2G8
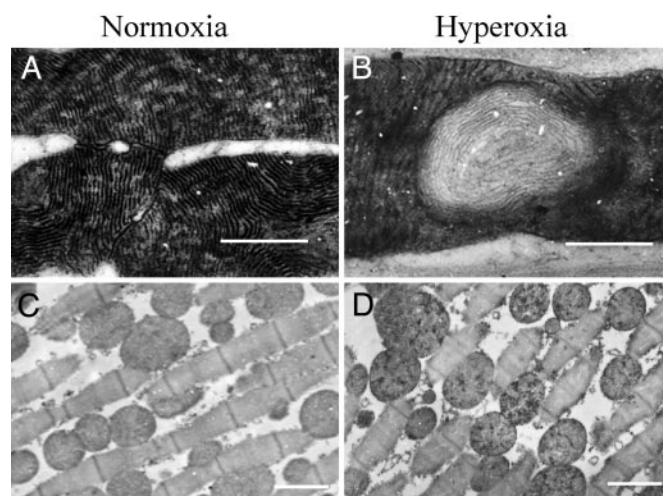

Fig. 3. Exposure to hyperoxia induces defects in complex IV of the electron transport chain. (*A*) Electron micrograph of flight muscle (*white^{1118}* strain) showing staining for COX activity. After 6 days under normoxia, mitochondria stain uniformly. (*B*) After 6 days under hyperoxia, cristae within a swirl are COX deficient (COX⁻), whereas cristae in the remainder of the mitochondrion are COX⁺. (*C*) Electron micrograph of flight muscle from control flies maintained under normoxia and stained with mAb 2G8, which specifically recognizes the apoptogenic cytochrome *c* epitope. No immunoreactivity is seen. (*D*) After exposure to hyperoxia for 4 days, the preapoptotic epitope for mAb 2G8 is exposed. (Scale bars indicate 1 μm.)
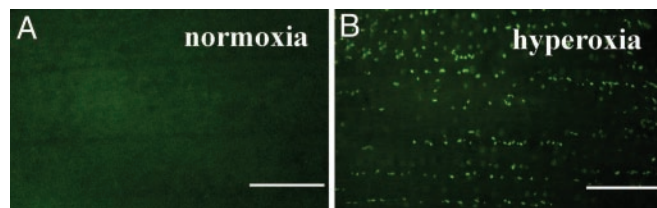

Fig. 4. Apoptosis induced in the flight muscle by hyperoxia. (*A*) Flight muscle from a control fly, maintained under normoxia for 4 days, exhibits no TUNEL-positive nuclei, whereas flies exposed to hyperoxia for 4 days (*B*), and assayed by TUNEL staining 2 days later, have many apoptotic nuclei (green). (Scale bars indicate 100 μm.)

specifically recognizes the apoptogenic cytochrome *c* display (43). To examine the effects of oxygen stress on cytochrome *c* conformation, flight muscle from flies exposed to hyperoxia and control flies maintained under normoxia were stained with mAb 2G8. As shown in Fig. 3*C*, flight muscle from control flies did not display immunoreactivity with mAb 2G8. However, pronounced exposure of the epitope for mAb 2G8 was observed in flight muscle of flies that had been exposed to oxygen stress for 4 days (Fig. 3*D*). Because this alteration has been reported to precede programmed cell death during *Drosophila* development (42), we examined the flight muscle by means of *in situ* TUNEL staining, which is a method that detects a nuclear hallmark of apoptosis. Although control flies maintained for 5 days under normoxia did not display TUNEL-positive nuclei (Fig. 4*A*), the flight muscle of flies exposed to hyperoxia for 5 days showed an abundance of TUNEL-positive nuclei (Fig. 4*B*), suggesting that mitochondrial dysfunction results ultimately in cell death through an apoptotic mechanism.

Age-related changes to mitochondrial morphology have been reported (44, 45), including enlargement, matrix vacuolization, shortened cristae, and crista-free regions. A strikingly similar pathology to swirls has been described (46) in the flight muscle of very old blowflies (46). We examined mitochondrial structure as a function of age in *white^{1118}*, which at 25°C in normoxia has a mean lifespan of ≈40 days and a maximum lifespan of ≈65 days. In young flies (<12 days of age), few swirls were observed. In old flies (≥56 days of age), mitochondrial swirls were widespread throughout the flight muscle. The observation that hyperoxia accelerates the accumulation of swirls is consistent with the idea that swirls arise as a result of oxidative stress.

To observe the 3D structure of swirls, we examined 0.08-μm serial sections through entire mitochondria. Fig. 5 shows such a series. The pattern varies strikingly with the plane of section. Whereas, in a given plane, a swirl may appear self-contained, the full series shows that the rearranged cristae include "projections" that appear to span the outer membrane of the mitochondrion. Serial sections through five additional mitochondria revealed similar projections to the outer membrane in all cases. It is remarkable that the remainder of the mitochondrion can remain otherwise apparently intact. This phenomenon may be understood in terms of the observations of Frey and Mannella (47), who suggest that the cristae in a mitochondrion are contained in relatively autonomous compartments.

The previously identified long-lived mutant *mth* is resistant to several extrinsic stressors, including the *in vivo* superoxide generator paraquat (37). We tested the ability of *mth* mutants to withstand hyperoxia and discovered that *mth* displayed increased survival compared with parental and WT controls (Fig. 6). This observation suggested that a genetic screen could yield relevant mutants. We, therefore, screened ≈1,000 lines containing *P*-element insertions in a *white^{1118}* background for altered survival under hyperoxia. This yielded a set of mutants
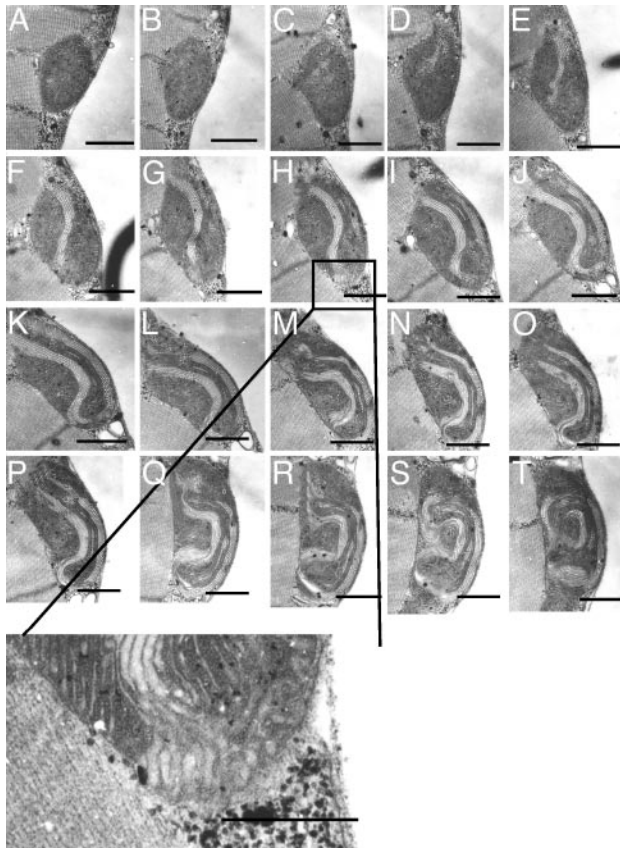
Walker and Benzer

Fig. 5. Serial sections through a mitochondrion containing a swirl. (*A–T*) Electron micrographs of flight muscle of *Drosophila* (*white^1118* strain), after 4 days under hyperoxia. Section thickness is 0.08 μm. Higher magnification of boxed region in *H* shows projection of swirl to the outer membrane. (Scale bars indicate 1 μm.)

with increased resistance to oxygen and others with hypersensitivity. Although the parental line *white^1118* displays a mean survival of 6.9 ± 0.1 days under hyperoxia, we isolated several lines that display unusually high sensitivity (<2 days mean survival). Such short-lived mutants are of particular interest because they may identify genes that are normally necessary to protect against endogenous oxidative stress. To test whether any of the disrupted genes are important in maintaining the
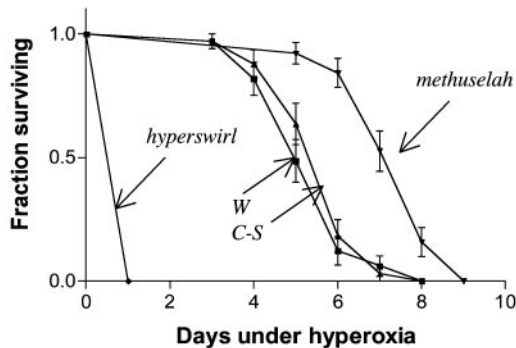

Fig. 6. The long-lived *mth* mutant displays resistance to oxygen stress whereas *hys* is hypersensitive. Survival curves (± SE) under hyperoxia of *mth* mutant males compared with its parental line, *white^1118* and the WT strain Canton-S (*C-S*). The *mth* displays increased resistance to hyperoxia (log-rank test; $P < 0.0001$). The *hys* is extremely sensitive to hyperoxia (log-rank test; $P < 0.0001$).
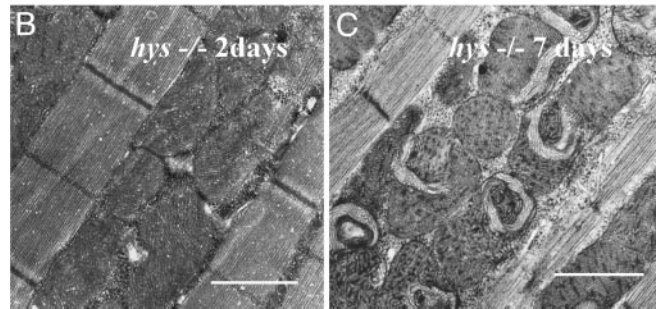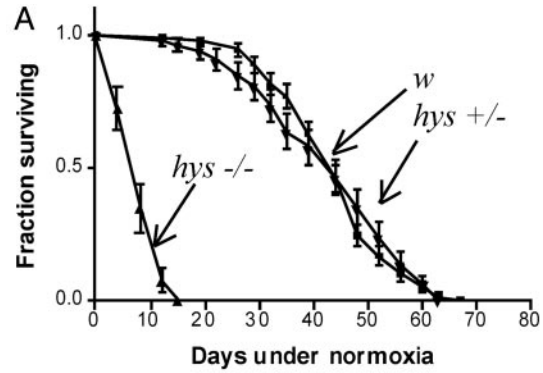
Fig. 7. The recessive mutant *hys* is short-lived and rapidly accumulates swirls. (*A*) Survival curves (±SE) of *white^1118* (*w*), *hys* heterozygotes (*hys*+/−), and homozygotes (*hys*−/−). Flies were maintained at 25°C, transferred every 2–4 days, and scored for survival. The *hys* homozygotes are very short-lived even under normoxia (log-rank test; $P < 0.0001$). (*B*) Electron micrograph of flight muscle of *hys* maintained under normoxic conditions for 2 days at 25°C. (*C*) Flight muscle of *hys* maintained under normoxic conditions for 7 days at 25°C. (Scale bars indicate 1 μm.)

integrity of the mitochondria, these mutants were examined by electron microscopy to identify those with mitochondrial degeneration.

We describe here the results for one of these mutants, *hys*, which is dramatically short-lived under hyperoxia (100% mortality in 1 day; Fig. 6). Under normoxia, flies of the *w^1118* parental strain live for ≈2 months at 25°C. In contrast, *hys* homozygous mutants display a twitching phenotype a few days after eclosion and then begin to die. Within 2 weeks, all are dead (mean survival of 8.4 ± 3.5 days; Fig. 7*A*). The gene is recessive; heterozygous flies live a normal lifespan. The flight muscle of *hys* homozygotes was examined at various ages under normoxia. At 2 days of age, *hys* mutants do not display major defects in the flight muscle mitochondria (Fig. 7*B*), but by 7 days they accumulated swirls throughout the flight muscle (Fig. 7*C*). To assay for possible functional correlates of the mitochondrial structural changes in *hys*, we assayed for gross metabolic alterations. The metabolic rate of *hys* was compared with the parental line, *white^1118* and the WT *Canton-S*. CO_2 production was measured in three groups of 10 flies. At 7 days of age, *hys* displays a 31% decrease in mean CO_2 production (Fig. 8*A*), consistent with severe mitochondrial dysfunction. To test for physiological correlates of mitochondrial dysfunction, we tested the ability of *hys* mutants to fly by using a simple flight assay (40). Whereas WT flies performed well in this assay (Fig. 8*B*), 2-day-old *hys* mutants display a severe defect in flight capacity (Fig. 8*C*).

By using genetic and molecular techniques, we discovered that the *P*-element insertion in this line is not responsible for the mutant phenotype; precise excision of the *P* element does not

CELL BIOLOGY

Fig. 8. The *hys* mutant displays respiratory and flight defects. (*A*) CO_2 production was measured for *white^1118*, the WT strain Canton-S (*C-S*), and the mutant *hys* after 7 days under normoxia. The mutant *hys* displays a 31% decrease in metabolic rate ($P < 0.001$). (*B*) Flight ability was measured in a simple flight assay, as described (40). In brief, control (*C-S*) flies wer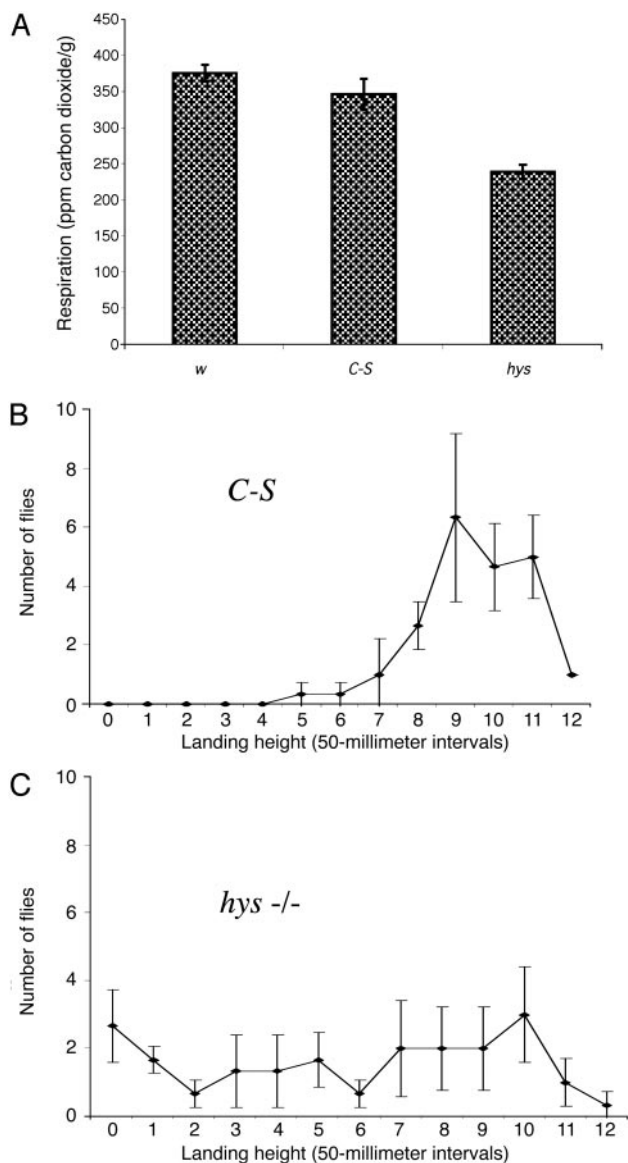e dropped into a 500-ml graduated cylinder with its internal walls coated with paraffin oil. Normal flies quickly initiate horizontal flight, striking the wall close to the entry level, whereas poor fliers land at lower levels or at the bottom of the cylinder. (*C*) The *hys* mutants (2 days old) perform poorly.

revert the phenotype. We mapped the *hys* mutation by using a multiply marked second chromosome. The recombination data placed the mutation in the central region of the chromosome, near the centromere. Molecular cloning of the *hys* gene and characterization of the associated pathways may identify primary targets of age-related mitochondrial dysfunction.

Discussion

In the past decade, considerable progress has been made toward understanding the genetic regulation of longevity (48–50). At the same time, we know relatively little with regard to the proximal targets of the aging process. In *C. elegans*, a progressive deterioration of muscle has been reported with age (51), but the underlying molecular mechanisms remain unknown. Several investigators have proposed that accumulation of damage to macromolecules within the mitochondrion determines the rate of aging (3). Therefore, understanding the molecular mechanisms involved in age-related mitochondrial decay is of particular importance. *Drosophila* has proven to be an invaluable resource for understanding many molecular and cellular mechanisms of human disease, powered by versatile gene discovery methods and a biology that has much in common with that of humans. We have examined the pathological consequences of oxygen stress on adult *Drosophila*. In doing so, we have discovered a biomarker of oxidative damage to the mitochondria within the flight muscle. Swirls may represent an early event in the deterioration of the mitochondrion. The unusually close packing of cristae in the flight muscle mitochondria makes it possible to detect this early event. Also, insect flight muscle is reported to be the most metabolically active tissue known (52). However, analysis of leg muscle of flies exposed to hyperoxia revealed a similar pathology, indicating that this phenotype is not specific to the flight muscles. We found that the defect is associated with a localized loss of COX activity and a conformational change of cytochrome *c*. Under oxygen stress, widespread apoptosis in the flight muscle is observed, suggesting that the rearrangement of the cristae is responsible for the induction of apoptosis by a change in cytochrome *c*. In mammalian cells, changes to mitochondrial ultrastructure after treatment with a proapoptotic member of the Bcl-2 family, called Bid, have been described (53). These findings suggest a structural reorganization of the cristae, reminiscent of swirls, which acts to mobilize the cristae stores of cytochrome *c* during apoptosis.

We have developed a paradigm using hyperoxia for identifying nuclear-encoded genes that are important in maintaining the integrity of the mitochondrion with age. In a relatively small screen, we have identified *hys*, which displays a rapid decline in mitochondrial respiration and muscle function. Several lines of evidence implicate mitochondrial dysfunction in various neurodegenerative diseases (25), and future work could possibly focus on examining the consequences of mitochondrial dysfunction on the nervous system in this mutant. Identifying genetic modifiers of *hys* will reveal the key molecular mediators of the pathogenesis resulting from mitochondrial dysfunction. Finding methods to prevent the accumulation of swirls in *hys*, either by overexpression of the normal gene or by stimulating its expression with appropriate drugs, may lead to methods of lifespan extension and effective therapeutic tools to counteract human diseases that result from mitochondrial dysfunction.

1. Harman, D. (1957) *J. Gerontol.* **2,** 298–300.
2. Sohal, R. S. & Weindruch, R. (1996) *Science* **273,** 59–63.
3. de Grey, A. D. (1999) *The Mitochondrial Free Radical Theory of Aging* (RG Landes, Austin, TX).
4. Finkel, T. & Holbrook, N. J. (2000) *Nature* **408,** 239–247.
5. Marnett, L. J., Hurd, H. K., Hollstein, M. C., Levin, D. E., Esterbauer, H. & Ames, B. N. (1985) *Mutat. Res.* **148,** 25–34.
6. Fraga, C. G., Shigenaga, M. K., Park, J. W., Degan, P. & Ames, B. N. (1990) *Proc. Natl. Acad. Sci. USA* **87,** 4533–4537.
7. Stadtman, E. R. (1992) *Science* **257,** 1220–1224.
8. Levine, R. L. & Stadtman, E. R. (2001) *Exp. Gerontol.* **36,** 1495–1502.
9. Lithgow, G. J. & Walker, G. A. (2002) *Mech. Ageing Dev.* **123,** 765–771.
10. Hekimi, S. & Guarente, L. (2003) *Science* **299,** 1351–1354.

11. Melov, S., Ravenscroft, J., Malik, S., Gill, M. S., Walker, D. W., Clayton, P. E., Wallace, D. C., Malfroy, B., Doctrow, S. R. & Lithgow, G. J. (2000) *Science* **289,** 1567–1569.
12. Sun, J., Folk, D., Bradley, T. J. & Tower, J. (2002) *Genetics* **161,** 661–672.
13. Orr, W. C. & Sohal, R. S. (1994) *Science* **263,** 1128–1130.
14. Parkes, T. L., Elia, A. J., Dickinson, D., Hilliker, A. J., Phillips, J. P. & Boulianne, G. L. (1998) *Nat. Genet.* **19,** 171–174.
15. Sun, J. & Tower, J. (1999) *Mol. Cell. Biol.* **19,** 216–228.
16. Seto, N. O., Hayashi, S. & Tener, G. M. (1990) *Proc. Natl. Acad. Sci. USA* **87,** 4270–4274.
17. Shigenaga, M. K., Hagen, T. M. & Ames, B. N. (1994) *Proc. Natl. Acad. Sci. USA* **91,** 10771–10778.
18. Wallace, D. C. (1999) *Science* **283,** 1482–1488.
19. Harper, M. E., Monemdjou, S., Ramsey, J. J. & Weindruch, R. (1998) *Am. J. Physiol.* **275,** E197–E206.
20. Lee, C. M., Lopez, M. E., Weindruch, R. & Aiken, J. M. (1998) *Free Radical Biol. Med.* **25,** 964–972.
21. Schwarze, S. R., Weindruch, R. & Aiken, J. M. (1998) *Free Radical Biol. Med.* **25,** 740–747.
22. Cortopassi, G. A., Shibata, D., Soong, N. W. & Arnheim, N. (1992) *Proc. Natl. Acad. Sci. USA* **89,** 7370–7374.
23. Michikawa, Y., Mazzucchelli, F., Bresolin, N., Scarlato, G. & Attardi, G. (1999) *Science* **286,** 774–779.
24. Behl, C. & Moosmann, B. (2002) *Biol. Chem.* **383,** 521–536.
25. Beal, M. F. (2003) *Ann. N.Y. Acad. Sci.* **991,** 120–131.
26. Simon, D. K. & Johns, D. R. (1999) *Annu. Rev. Med.* **50,** 111–127.
27. Jamieson, D., Chance, B., Cadenas, E. & Boveris, A. (1986) *Annu. Rev. Physiol.* **48,** 703–719.
28. Gille, J. J. & Joenje, H. (1992) *Mutat. Res.* **275,** 405–414.
29. Fukui, K., Onodera, K., Shinkai, T., Suzuki, S. & Urano, S. (2001) *Ann. N.Y. Acad. Sci.* **928,** 168–175.
30. Honda, S., Ishii, N., Suzuki, K. & Matsuo, M. (1993) *J. Gerontol. B Psychol. Sci. Soc. Sci.* **48,** B57–B61.
31. Ishii, N., Fujii, M., Hartman, P. S., Tsuda, M., Yasuda, K., Senoo-Matsuda, N., Yanase, S., Ayusawa, D. & Suzuki, K. (1998) *Nature* **394,** 694–697.
32. Yan, L. J., Levine, R. L. & Sohal, R. S. (1997) *Proc. Natl. Acad. Sci. USA* **94,** 11168–11172.
33. Fenn, W., Henning, M & Philpott, M. (1967) *J. Gen. Physiol.* **50,** 1693–1707.
34. Williams, C. M. & Beecher, H. K. (1944) *Am. J. Physiol.* **140,** 566–573.
35. Philpott, D. E., Bensch, K. G. & Miquel, J. (1974) *Aerospace Med.* **45,** 283–289.
36. Botella, J. A., Ulschmid, J. K., Gruenewald, C., Moehle, C., Kretzschmar, D., Becker, K. & Schneuwly, S. (2004) *Curr. Biol.* **14,** 782–786.
37. Lin, Y. J., Seroude, L. & Benzer, S. (1998) *Science* **282,** 943–946.
38. Rorth, P., Szabo, K., Bailey, A., Laverty, T., Rehm, J., Rubin, G. M., Weigmann, K., Milan, M., Benes, V., Ansorge, W., *et al.* (1998) *Development (Cambridge, U.K.)* **125,** 1049–1057.
39. Nonaka, I., Koga, Y., Ohtaki, E. & Yamamoto, M. (1989) *J. Neurol. Sci.* **92,** 193–203.
40. Benzer, S. (1973) *Sci. Am.* **229(6),** 24–37.
41. Zamzami, N. & Kroemer, G. (2001) *Nat. Rev. Mol. Cell Biol.* **2,** 67–71.
42. Varkey, J., Chen, P., Jemmerson, R. & Abrams, J. M. (1999) *J. Cell Biol.* **144,** 701–710.
43. Dorstyn, L., Read, S., Cakouros, D., Huh, J. R., Hay, B. A. & Kumar, S. (2002) *J. Cell Biol.* **156,** 1089–1098.
44. Sohal, R. S. & Allison, V. H. (1971) *Exp. Gerontol.* **6,** 167–172.
45. Wilson, P. D. & Franks, L. M. (1975) *Adv. Exp. Med. Biol.* **53,** 171–183.
46. Sacktor, B. & Shimida, Y. (1972) *J. Cell Biol.* **52,** 465–477.
47. Frey, T. G. & Mannella, C. A. (2000) *Trends Biochem. Sci.* **25,** 319–324.
48. Guarente, L. & Kenyon, C. (2000) *Nature* **408,** 255–262.
49. Partridge, L. & Gems, D. (2002) *Nat. Rev. Genet.* **3,** 165–175.
50. Tatar, M., Bartke, A. & Antebi, A. (2003) *Science* **299,** 1346–1351.
51. Herndon, L. A., Schmeissner, P. J., Dudaronek, J. M., Brown, P. A., Listner, K. M., Sakano, Y., Paupard, M. C., Hall, D. H. & Driscoll, M. (2002) *Nature* **419,** 808–814.
52. Sacktor, B. (1970) *Adv. Insect Physiol.* **7,** 267–347.
53. Scorrano, L., Ashiya, M., Buttle, K., Weiler, S., Oakes, S. A., Mannella, C. A. & Korsmeyer, S. J. (2002) *Dev. Cell* **2,** 55–67.

CELL BIOLOGY